JOURNAL OF COLLOID AND INTERFACE SCIENCE **183,** 223–235 (1996)
ARTICLE NO. 0537

# Adsorption from Micellar Surfactant Solutions: Nonlinear Theory and Experiment

K. D. DANOV,* P. M. VLAHOVSKA,* T. HOROZOV,* C. D. DUSHKIN,*
P. A. KRALCHEVSKY,*,[1] A. MEHRETEAB,† AND GUY BROZE‡

*Laboratory of Thermodynamics and Physicochemical Hydrodynamics, Faculty of Chemistry, University of Sofia, 1126 Sofia, Bulgaria; †Colgate–Palmolive Technology Center, Piscataway, New Jersey 08854-5596; and ‡Colgate–Palmolive R&D, Inc., Avenue du Parc Industriel, B-4041 Milmort (Herstal), Belgium

Received January 30, 1996; accepted April 29, 1996

**A theoretical approach to the kinetics of adsorption on the expanding interface of a micellar surfactant solution is proposed. The nonlinear partial differential equations of mass transfer of the micelles and monomers are reduced to ordinary differential equations, which are solved numerically along with the nonlinearized adsorption isotherm as a boundary condition. Being more general, this theoretical approach is consistent also with the special case of small deviations from equilibrium widely used in the kinetics of micellization. The theory is applied further to fit the experimental data for dynamic surface tension of micellar solutions of sodium dodecyl sulfate and sodium polyoxyethylene-2 sulfate measured by the maximum bubble pressure (MBP) method. The expansion of the bubble surface is accounted for by using the experimental dependence of the bubble size on time. The calculated effective rate constant of micelle decay for sodium dodecyl sulfate turns out to be sensitive to the mechanism of the micelle's disintegration. This provides a possibility for one to determine the rate constants of the fast and slow processes in the relaxation kinetics of micellization by using a relatively simple experimental technique for dynamic surface tension measurement like the MBP method.** 

*Key Words:* **adsorption kinetics; micellar solution; dynamic surface tension; maximum bubble pressure method; sodium dodecyl sulfate.**

## 1. INTRODUCTION

The adsorption from surfactant solutions is a process inevitably accompanying any dynamic measurement of surface tension (1), surface elasticity, and viscosity (2). The theoretical treatment of this problem lies in solving the respective diffusion equation(s) under appropriate boundary conditions. In general, this is a nonlinear boundary problem. One source of nonlinearity is the relation between the subsurface concentration of surfactant monomers, $c_{10}$, and the surfactant adsorption, $\Gamma$. In the case of diffusion controlled adsorption it is usually assumed that the instantaneous values of $c_{10}$ and $\Gamma$ are connected by the equilibrium adsorption isotherm

$$c_{10} = c_{10}(\Gamma). \qquad [1.1]$$

For example, it can be the Langmuir adsorption isotherm

$$\frac{c_{10}(t)}{b} = \frac{\Gamma(t)}{\Gamma_\infty - \Gamma(t)}, \qquad [1.2]$$

where $b$ and $\Gamma_\infty$ are constants and $t$ denotes time. Both nonionic (3–5) and ionic (6) surfactants are found to comply with the Langmuir adsorption isotherm. More sophisticated adsorption isotherms are also used (7). In some particular cases (small adsorption, small deviations from equilibrium, etc.) the adsorption isotherm can be linearized and then standard mathematical methods can be applied to solve the diffusion problem, see e.g., Refs. (8–10). However, the general boundary problem is essentially nonlinear. One way to solve it is to use perturbation series methods (11). Another approach is to solve numerically the respective set of equations, including the partial differential equation of diffusion (12, 13). This method, although being in principle exact, is much more time consuming. A considerably simpler and less time consuming method was recently proposed (14). The latter method, which is analogous to the von Karman approach to the hydrodynamical boundary layer (see e.g., Ref. (15)), was successfully applied to the interpretation of data provided by the maximum bubble pressure technique for surfactant solutions below the critical micellization concentration (CMC). The present article is a natural extension of Ref. (14) to surfactant concentrations above CMC.

Since the micelles are unstable species, they can enhance essentially the transport of monomers from the bulk to the interface or backward. The studies on kinetics of micellization in homogeneous solutions reveal that the two relaxation processes take place for small deviations from equilibrium (16, 17). Correspondingly, their theoretical interpretation is based on linearization of the respective kinetic equations (16–18). More sophisticated is the diffusion problem in micellar solutions: both monomers and micelles are involved in diffusion accompanied with mass exchange between these

[1] To whom correspondence should be addressed.



0021-9797/96 $18.00

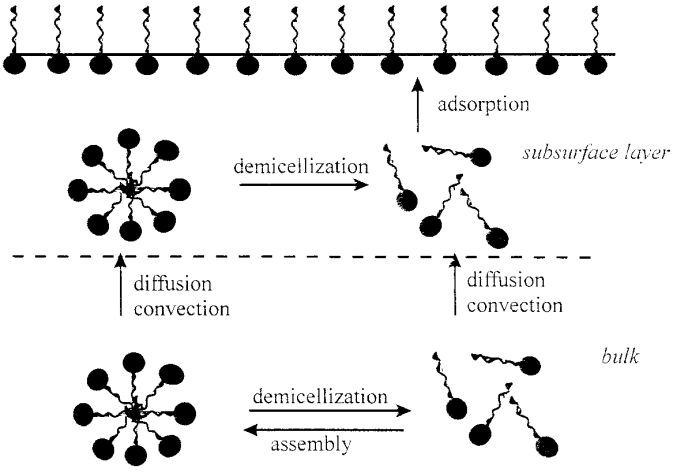


**FIG. 1.** Role of the micelles in the kinetics of surfactant adsorption. In the bulk the micelles exist in a dynamic equilibrium with the monomers. In the vicinity of an expanded adsorption monolayer the micelles release monomers in order to restore the equilibrium surfactant concentration on the surface and in the bulk.

two species, which can be described as a chemical reaction, see Fig. 1. Again the analytical solutions obtained are based on linearization for the case of small deviations from equilibrium (10, 19, 20). Fortunately, the extension of the approach developed in Ref. (14) allows us to solve also the latter problem in its general nonlinear form. The article is organized as follows.

First, we introduce the basic differential equations and the respective boundary conditions. Next, following the von Karman approach we introduce model concentration distribution. Then, we describe the procedure of calculation. Further, the theoretical predictions are compared with the experiment and discussed. Numerical comparison with an alternative theoretical approach is given in the Appendix.

## 2. BASIC EQUATIONS

Let us consider a uniform interface which is being subjected to expansion or compression. We assume that the rate of interfacial dilation

$$\dot{\alpha} = \frac{1}{A}\frac{dA}{dt} \qquad [2.1]$$

($A$ is area) is a known function of time. The interfacial dilation gives rise to a diffusion flux of surfactant in accordance with the equation

$$\frac{d\Gamma}{dt} + \alpha(t)\Gamma(t) = D_1 \left.\frac{\partial c_1}{\partial x}\right|_{x=0}, \qquad [2.2]$$

where $D_1$ is the monomer diffusivity, $c_1(x, t)$ is the monomer concentration; the plane $x = 0$ corresponds to the solution surface, and the $x$-axis is directed inward to the solution. Since, in general, the interfacial dilation is coupled with some convective flow in the bulk of the solution, the bulk monomer concentration obeys the equation of convective diffusion (8)

$$\frac{\partial c_1}{\partial t} + V_x \frac{\partial c_1}{\partial x} = D_1 \frac{\partial^2 c_1}{\partial x^2} + mk_d c_m - mk_a c_1^m, \qquad [2.3]$$

with $V_x$ being the $x$-component of the mean mass velocity; the last two terms in Eq. [2.3] express the source and drain of monomers due to the presence of micelles. In particular, $c_m$ is the concentration of the micelles, $m$ is their aggregation number, and $k_a$ and $k_d$ are the rate constants of the micellar assembly and disassembly:

$$A_m \underset{k_a}{\overset{k_d}{\leftrightarrow}} mA_1 \qquad [2.4]$$

(here $A_m$ and $A_1$ symbolize micelle and monomer). We restrict our considerations to the simplest possible reaction mechanism expressed by Eq. [2.4], which gives the overall surfactant mass balance in the reaction. We are aware of the fact that the real reaction mechanism can be much more complicated (16–21). On the other hand, Eq. [2.4] is found to reflect correctly the main features of micellization through the respective mass action law.

Analogously, one can write the diffusion equation for the micelles (8):

$$\frac{\partial c_m}{\partial t} + V_x \frac{\partial c_m}{\partial x} = D_m \frac{\partial^2 c_m}{\partial x^2} + k_a c_1^m - k_d c_m. \qquad [2.5]$$

Here $D_m$ is the diffusion coefficient of the micelles. Below we will consider the case when the surface dilation is isotropic. As proven by van Voorst Vader *et al.* (2), in this case

$$V_x = -x\dot{\alpha}(t). \qquad [2.6]$$

The boundary conditions are

$$c_1(0, t) = c_{10}(t), \quad \lim_{x\to\infty} c_1(x, t) = c_{1\infty} = \text{const} \qquad [2.7]$$

$$c_m(0, t) = c_{m0}(t), \quad \lim_{x\to\infty} c_m(x, t) = c_{m\infty} = \text{const} \qquad [2.8]$$

$$\lim_{x\to\infty} \frac{\partial c_1}{\partial x} = \lim_{x\to\infty} \frac{\partial c_m}{\partial x} = 0. \qquad [2.9]$$

$c_{m0}$ in Eq. [2.8] denotes the subsurface concentration of the micelles, while $c_{1\infty}$ and $c_{m\infty}$ stand for the bulk concentrations of surfactant monomers and micelles far from the surface. It should be noted that the micelles do not adsorb. Hence, the micellar flux at the interface must be zero (8), i.e.,

$$\left.\frac{\partial c_m}{\partial x}\right|_{x=0} = 0. \qquad [2.10]$$

Following the approach in Ref. (14) we introduce the quantities

$$l_1(t) = \frac{1}{c_{1\infty}} \int_0^\infty [c_{1\infty} - c_1(x, t)]dx \qquad [2.11]$$

$$l_m(t) = \frac{1}{c_{m\infty}} \int_0^\infty [c_{m\infty} - c_m(x, t)]dx. \qquad [2.12]$$

$l_1$ represents the thickness of an imaginary layer adjacent to the interface, which contains an amount of free monomers (of uniform concentration $c_{1\infty}$) equal to the deficiency of monomers in a vicinity of the real interface caused by the surfactant adsorption. $l_m$ has analogous meaning. Next, let us integrate Eq. [2.3] from $x = 0$ to $x = \infty$; thus in keeping with Eqs. [2.6], [2.11], and the boundary conditions [2.7] and [2.9] we derive

$$\frac{dl_1}{dt} + \dot{\alpha} l_1 = \frac{1}{c_{1\infty}} \left[ D_1 \left.\frac{\partial c_1}{\partial x}\right|_{x=0} - m \int_0^\infty (k_d c_m - k_a c_1^m)dx \right]. \qquad [2.13]$$

Similarly, from Eqs. [2.5], [2.6], and [2.8]–[2.10] it follows that

$$\frac{dl_m}{dt} + \dot{\alpha} l_m = \frac{1}{c_{m\infty}} \int_0^\infty (k_d c_m - k_a c_1^m)dx. \qquad [2.14]$$

The elimination of the integral term between Eqs. [2.13] and [2.14] leads to an expression for $(\partial c_1/\partial x)_{x=0}$, which upon substitution in Eq. [2.2] yields

$$\frac{d\Gamma}{dt} + \dot{\alpha}\Gamma = c_{1\infty}\left(\frac{dl_1}{dt} + \dot{\alpha} l_1\right) + m c_{m\infty}\left(\frac{dl_m}{dt} + \dot{\alpha} l_m\right). \qquad [2.15]$$

Having in mind Eq. [2.1] one can easily integrate Eq. [2.15]. To determine the integration constants initial conditions are necessary. We set

$$A(0) = A_0, \quad \Gamma(0) = \Gamma_0, \quad l_1(0) = l_m(0) = 0. \qquad [2.16]$$

To have $l_1(0) = l_m(0) = 0$ we have supposed that the initial moment $t = 0$ corresponds to a disturbance of the interface at nondisturbed uniform bulk concentrations $c_1 \equiv c_{1\infty}$ and $c_m \equiv c_{m\infty}$, cf., Eqs. [2.11] and [2.12]. From Eqs. [2.15] and [2.16] one finally obtains

$$\Gamma(t) = \frac{A_0}{A(t)} \Gamma_0 + c_{1\infty} l_1(t) + m c_{m\infty} l_m(t). \qquad [2.17]$$

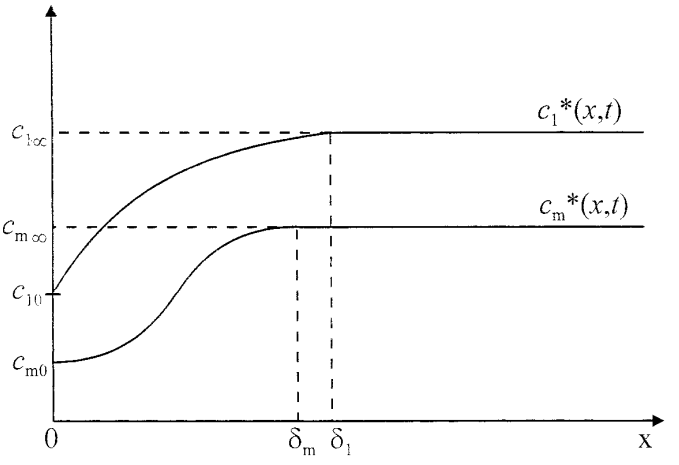


**FIG. 2.** Sketch of the model concentration profiles, Eqs. [3.1] and [3.2], for free monomers and micelles (the air/water interface is located at $x = 0$).

## 3. MODELING OF THE CONCENTRATION PROFILES

Equation [2.17] calls for some discussion. First of all we recall that we are interested in the time dependence of the interfacial properties (adsorption, surface tension, etc.). Second, Eq. [2.17] implies that the instantaneous adsorption, $\Gamma(t)$, depends on two *integrals*, $l_1(t)$ and $l_m(t)$, of the concentration profiles $c_1(x, t)$ and $c_m(x, t)$, see Eqs. [2.11] and [2.12]. In other words, we need to know these integrals, rather than the detailed information about the values of $c_1$ and $c_m$ at every point $x$. This fact enables one to use model profiles for $c_1(x)$ and $c_m(x)$ possessing appropriate integral properties, instead of the exact solutions of the respective diffusion equations (14, 15). For $c_1$ we will use the same model profile as in Ref. (14)

$$c_1^*(x, t) = c_{10}(t) + [c_{1\infty} - c_{10}(t)]\sin\frac{\pi x}{2\delta_1} \quad \text{for } x \leqslant \delta_1 \qquad [3.1]$$

$$c_1^*(x, t) = c_{1\infty} = \text{const} \quad \text{for } x \geqslant \delta_1,$$

where $\delta_1(t)$ is a function which will be determined below. As seen in Fig. 2, Eq. [3.1] determines $c_1^*$ as a smooth monotonic function satisfying the boundary conditions [2.7]. The new step is the introduction of model profile for $c_m$ as

$$c_m^*(x, t) = \frac{1}{2}[c_{m\infty} + c_{m0}(t)] - \frac{1}{2}[c_{m\infty} - c_{m0}(t)]\cos\frac{\pi x}{\delta_m}$$

$$\text{for } x \leqslant \delta_m \quad [3.2]$$

$$c_m^*(x, t) = c_{m\infty} = \text{const for } x \geqslant \delta_m,$$

see Fig. 2. One check that Eq. [3.2] determines $c_m^*$ as a smooth monotonic function satisfies the boundary conditions [2.8]–[2.10].

Equation [3.1] contains two unknown functions of time, $c_{10}(t)$ and $\delta_1(t)$. To determine them we impose two conditions for equivalence between the model and real *monomer* concentration distributions

$$\int_0^\infty [c_{1\infty} - c_1^*(x, t)]dx = \int_0^\infty [c_{1\infty} - c_1(x, t)]dx \quad [3.3]$$

$$\left.\frac{\partial c_1^*}{\partial x}\right|_{x=0} = \left.\frac{\partial c_1}{\partial x}\right|_{x=0}. \quad [3.4]$$

In particular, the last equation implies that the diffusion flux at the interface in the model system must be the same as in the real system. By substituting Eqs. [2.11] and [3.1] into Eq. [3.3] one derives

$$c_{1\infty} l_1(t) = \frac{\pi - 2}{\pi}[c_{1\infty} - c_{10}(t)]\delta_1(t). \quad [3.5]$$

Further, by means of Eqs. [3.1], [3.4], and [3.5] one obtains

$$\left.\frac{\partial c_1}{\partial x}\right|_{x=0} = \frac{\pi - 2}{2c_{1\infty} l_1(t)}[c_{1\infty} - c_{10}(t)]^2. \quad [3.6]$$

In analogy with Eqs. [3.3] and [3.4] we impose two conditions for equivalence between the model and real *micellar* concentration distributions

$$\int_0^\infty [c_{m\infty} - c_m^*(x, t)]dx = \int_0^\infty [c_{m\infty} - c_m(x, t)]dx \quad [3.7]$$

$$\left.\frac{\partial^2 c_m^*}{\partial x^2}\right|_{x=0} = \left.\frac{\partial^2 c_m}{\partial x^2}\right|_{x=0}. \quad [3.8]$$

The derivatives $\partial c_m/\partial x$ and $\partial c_m^*/\partial x$ for $x = 0$ are both equal to zero, cf., Eqs. [2.10] and [3.2]; that is the reason why Eq. [3.8] imposes equality of the second derivatives. From Eqs. [2.12], [3.2], and [3.7] one derives an analogue of Eq. [3.5]

$$c_{m\infty} l_m(t) = \tfrac{1}{2}[c_{m\infty} - c_{m0}(t)]\delta_m(t). \quad [3.9]$$

In addition, from Eqs. [2.5], [2.6], [3.2], and [3.8] one obtains

$$\frac{dc_{m0}}{dt} = \frac{\pi^2 D_m}{2\delta_m^2}[c_{m\infty} - c_{m0}(t)] - k_d c_{m0}(t) + k_a c_{10}^m(t). \quad [3.10]$$

Next, let us consider the integral in Eqs. [2.13] and [2.14]. Having in mind that $k_d c_{m\infty} = k_a c_{1\infty}^m$, we represent this integral in the form

$$Q(t) = \int_0^\infty \{k_a[c_{1\infty}^m - c_1^m(x, t)] - k_d[c_{m\infty} - c_m(x, t)]\}dx. \quad [3.11]$$

The substitution of $c_1^*$ for $c_1$ in Eq. [3.11], along with Eqs. [2.12] and [3.1], yields

$$Q(t) = \frac{2}{\pi} k_a c_{1\infty}^m \delta_1(t) G_m\left(\frac{c_{10}(t)}{c_{1\infty}}\right) - k_d c_{m\infty} l_m(t), \quad [3.12]$$

where

$$G_m(\xi) \equiv \int_0^{\pi/2} \{1 - [\xi + (1 - \xi)\sin\omega]^m\}d\omega. \quad [3.13]$$

In view of Eqs. [3.6] and [3.11] one can transform Eqs. [2.13] and [2.14] to read

$$\frac{dl_1}{dt} + \dot{\alpha} l_1 = \frac{(\pi - 2)D_1}{2l_1}\left(1 - \frac{c_{10}}{c_{1\infty}}\right)^2 - \frac{m}{c_{1\infty}} Q(t) \quad [3.14]$$

$$\frac{dl_m}{dt} + \dot{\alpha} l_m = \frac{1}{c_{m\infty}} Q(t), \quad [3.15]$$

where $Q(t)$ is given by Eq. [3.12].

In summary, we have a set of seven equations, Eqs. [1.1], [2.17], [3.5], [3.9], [3.10], [3.14], and [3.15], for determining seven unknown functions: $\Gamma(t)$, $c_{10}(t)$, $c_{m0}(t)$, $l_1(t)$, $l_m(t)$, $\delta_1(t)$, and $\delta_m(t)$. This set includes four algebraic equations and three ordinary differential equations of the first order. We solve this problem numerically. In general, it is a comparatively simple computational problem. In the next section we describe the procedure of calculations, which turns out to be extremely fast and well convergent. The reader who is not interested in the computational details may skip the next section and continue with Section 5, where the comparison of theory and experiment is presented.

## 4. PROCEDURE OF CALCULATIONS

### 4.1. Introduction of Dimensionless Variables

Let $\Gamma_e$ be the equilibrium surfactant adsorption and $T$ be some characteristic time of the process. (For example, if the maximum bubble pressure method (22–24) is used, $T$ can be the period of bubble release.) Then we introduce the dimensionless variables

$$\xi_1 = \frac{c_{10}}{c_1}, \quad \xi_m = \frac{c_{m0}}{c_m}, \quad \gamma = \frac{\Gamma}{\Gamma_e}, \quad \gamma_0 = \frac{\Gamma_0}{\Gamma_e} \quad [4.1]$$

$$x_1 = \frac{c_{1\infty}}{\Gamma_e} l_1, \quad x_m = \frac{mc_{m\infty}}{\Gamma_e} l_m, \quad \tau = \frac{t}{T} \quad [4.2]$$

$$y_1 = \frac{c_{1\infty}}{\Gamma_e} \delta_1, \quad y_m = \frac{mc_{m\infty}}{\Gamma_e} \delta_m, \quad a = \frac{A}{A_0} \quad [4.3]$$

$$d_1 = \sqrt{D_1 T} c_{1\infty}/\Gamma_e, \quad k = mc_{m\infty}/c_{1\infty} \quad [4.4]$$

$$d_m = \sqrt{D_m T} mc_{m\infty}/\Gamma_e, \quad v = k_d T. \quad [4.5]$$

The dimensionless form of Eq. [2.17] reads

$$\gamma = x_1 + x_m + \gamma_0/a \quad [4.6]$$

Similarly, Eqs. [3.5] and [3.9] can be transformed to read

$$x_1 = \frac{\pi - 2}{\pi} (1 - \xi_1) y_1 \quad [4.7]$$

$$x_m = \frac{1}{2} (1 - \xi_m) y_m. \quad [4.8]$$

Further, Eq. [3.10] takes the form

$$\frac{d\xi_m}{d\tau} = \frac{\pi^2 d_m^2}{2y_m^2} (1 - \xi_m) - v(\xi_m - \xi_1^m). \quad [4.9]$$

Finally, in view of Eq. [2.1] one can transform Eqs. [3.14] and [3.15] to read

$$\frac{d}{d\tau} (a^2 x_1^2) = (\pi - 2) a^2 d_1^2 (1 - \xi_1)^2 + 2va^2 x_1 \left[ x_m - \frac{2}{\pi} k y_1 G_m(\xi_1) \right] \quad [4.10]$$

$$\frac{d}{d\tau} (a^2 x_m^2) = -2va^2 x_m \left[ x_m - \frac{2}{\pi} k y_1 G_m(\xi_1) \right]. \quad [4.11]$$

The integral $G_m$ is given by Eq. [3.13]. This integral is a function of $\xi_1$ for a given value of $m$. We tabulated the values of the function $G_m$ vs $\xi_1$ ($0 \leqslant \xi_1 \leqslant 1$) and used these values in any subsequent numerical calculations. It should be noted that $G_m(1) = 0$ and that in a vicinity of the point $\xi_1 = 1$ the function $G_m(\xi_1)$ changes fast, see Fig. 3. For $\xi_1 < 1$ $G_m(\xi_1)$ levels off to $G_m(0)$. Physically $G_m(\xi_1)$ characterizes the micelles of aggregation number $m$ as sources of monomers depending on the deviation from equilibrium characterized by the parameter $\xi_1$.

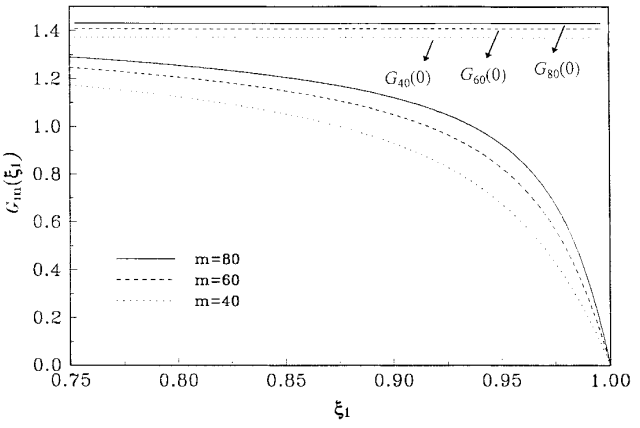


**FIG. 3.** Plot of the special function $G_m(\xi_1)$, Eq. [3.13], for three different values of the aggregation number: $m = 40$, 60, and 80.

### 4.2. Numerical Method

Our purpose is to solve the nonlinear system of Eqs. [4.6]–[4.11]. The most appropriate method for this problem is the method of the explicit differential schemes applied to the differential Eqs. [4.9]–[4.11]. This method requires a closer inspection of the behavior of the system for small times, because for $\tau \to 0$, $y_m \to 0$, and Eq. [4.9] exhibits a singularity. To elucidate this point we first ascribe an initial value

$$\xi_1^{(0)} = c_{10}^{(0)}/c_{1\infty} \quad [4.12]$$

to the dimensionless parameter $\xi_1$. Next, we choose a small time increment $\Delta\tau$ such to obey the relations

$$\Delta\tau \ll 1, \quad v\Delta\tau \ll 1, \quad kv\Delta\tau \ll 1. \quad [4.13]$$

Then the explicit differential scheme of Eq. [4.10] leads to

$$x_1 = \frac{1}{a} \sqrt{\pi - 2} d_1 (1 - \xi_1^{(0)}) \sqrt{\Delta\tau}. \quad [4.14]$$

As an explicit differential scheme is not applicable to Eq. [4.11], we apply to this equation an implicit differential scheme to obtain

$$x_m = \frac{4}{\pi} vky_1 G_m(\xi_1) \Delta\tau. \quad [4.15]$$

In Eq. [4.15] $y_1$ and $\xi_1$ are unknown. To determine them we first note that for $\tau \to 0$ one has $y_1 \sim x_1$, cf., Eq. [4.7], and then from Eqs. [4.13] and [4.15] it follows that $x_m \ll x_1$. Consequently, Eq. [4.6] reduces to

$$\gamma = x_1 + \gamma_0/a \quad (\tau \to 0). \tag{4.16}$$

Further we proceed as follows:

(1) Knowing the adsorption isotherm, that is Eq. [1.1] in dimensionless form, we substitute $\gamma$ from Eq. [4.16] to obtain the value of $\xi_1$.
(2) From Eq. [4.7] we determine $y_1$.
(3) With the above value of $\xi_1$ we calculate $G_m(\xi_1)$.
(4) Finally, from Eq. [4.15] we determine $x_m$.

Two quantities still remain unknown, viz., $\xi_m$ and $y_m$. To determine them we present Eq. [4.9] in the form

$$\frac{d}{d\tau}(1-\xi_m) + \frac{\pi^2 d_m^2}{2y_m^2}(1-\xi_m) + v(1-\xi_m) = v(1-\xi_1^m). \tag{4.17}$$

Then we apply an explicit differential scheme to Eq. [4.17] and use Eqs. [4.8] and [4.13]. The result reads

$$\frac{\pi^2 d_m^2 \Delta\tau^3}{8x_m^2} p^3 + p - v(1-\xi_1^m) = 0, \tag{4.18}$$

where

$$p = (1-\xi_m)/\Delta\tau. \tag{4.19}$$

From Eqs. [4.7], [4.14], and [4.15] it follows that

$$x_1 \sim \sqrt{\Delta\tau}, \quad y_1 \sim \sqrt{\Delta\tau}, \quad x_m \sim (\Delta\tau)^{3/2} \quad (\tau \to 0),$$

respectively. Hence, the coefficient multiplying $p^3$ in Eq. [4.18] tends to a finite constant for $\tau \to 0$. Further, one can check that the cubic equation for $p$, Eq. [4.18], has a single real solution for $p$, which is, moreover, always positive; this solution reads

$$p = [q_1 - (q_1^2 + q_2^3)^{1/2}]^{1/3} + [q_1 + (q_1^2 + q_2^3)^{1/2}]^{1/3}, \tag{4.20}$$

where

$$q_1 = \frac{4x_m^2 v(1-\xi_1^m)}{\pi^2 d_m^2 \Delta\tau^3}, \quad q_2 = \frac{8x_m^2}{3\pi^2 d_m^2 \Delta\tau^3}. \tag{4.21}$$

From [4.19] and [4.20] one determines $\xi_m$, which is then substituted in [4.8] to find $y_m$.

Thus, we determined the values of all variables in the time moment $\tau = \Delta\tau$. Further, these values serve as initial conditions to start any explicit method for solving the differential equations, Eqs. [4.9]–[4.11]. Note that at each step of the numerical integration we determine $\xi_1$ from Eq. [4.6] (in conjunction with the dimensionless Eq. [1.1]), $y_1$ from Eq. [4.7], and $y_m$ from Eq. [4.8]. As already mentioned the numerical procedure is extremely fast and well convergent.

Finally, we discuss a peculiarity of the computational procedure related to the fact that after a certain time moment, $\tau = \tau_e$, the adsorption acquires its equilibrium value, i.e., $\gamma = 1$ is the framework of some reasonable accuracy, see Eq. [5.4] below. Therefore, the numerical procedure for $\tau > \tau_e$ must be changed. In this case since $\xi_1$ cannot be obtained from adsorption isotherm the solved set of equations is modified as follows.

After substituting $\gamma$ with 1 in Eq. [4.6] one obtains

$$a = ax_1 + ax_m + \gamma_0. \tag{4.22}$$

Differentiating [4.22] by time, substituting $(d(ax_1))/(d\tau)$ and $(d(ax_m))/(d\tau)$ from Eq. [4.10] and [4.11], the equation describing changes of the subsurface concentration $\xi_1$ with time is obtained:

$$\xi_1 = 1 - \sqrt{\frac{\pi}{\pi - 2}\frac{x_1}{ad_1^2}\left(\frac{da}{d\tau}\right)}. \tag{4.23}$$

The final set of equations now consists of [4.22], [4.23], and unchanged [4.7]–[4.9], [4.11].

## 5. COMPARISON OF THEORY AND EXPERIMENT

### 5.1. Experimental Method

Below we compare the theory with experimental data obtained by means of the MBP method (22–24). This method allows a quick extension of a fluid–gas interface and detection of the dynamic surface tension $\sigma$ during time intervals ranging typically from 0.01 to 10 s. There are some peculiarities of the MBP method which are not always taken into account in the relevant theoretical models of the dynamic surface tension. The most important feature is that the full time dependence of $\sigma(t)$ is composed in fact by experimental points corresponding to different bubbles, i.e., interfaces, of different individual life times $t$ (24). Besides, within one bubble period the interfacial area does not remain constant throughout the adsorption process because the bubble surface expands appreciably which can lead to additional deviations from the equilibrium concentrations, at least in the vicinity of bubble surface. In contrast to these observations, MBP data were interpreted until now by theoretical models which are valid strictly for a single nonexpanding interface (9, 22, 25) or at small deviations from equilibrium (26). Although these approaches are not entirely unfounded, bearing in mind their application for solutions without micelles

(see, e.g., Refs. (27, 28)), one needs a higher degree of consistency between theory and experiment to make more decisive conclusions for the micellization kinetics.

Our theoretical approach avoids most of the contradictions between theory and experiment mentioned above. First, there is no assumption for small deviations from equilibrium which makes the model applicable to experimental methods like the MBP method, where the initial perturbation sometimes creates an almost clean interface. Second, we take into account the expansion of the interface in the course of adsorption which can lead effectively to an increase of the surface tension $\sigma$ (decrease of the adsorption) although the dominating trend is to lower $\sigma$ with time due to an increase of the adsorption. Third, as we know the exact law of bubble expansion, we integrate the respective equations for individual bubbles and combine them in a composite solution for $\sigma(t)$.

### 5.2. *Effect of the Micelles on the Surface Tension*

Our main purpose below is to compare our solution of the diffusion–adsorption problem with the experiment. To be sure that a possible difference between theory and experiment is not a consequence of the usage of an improper adsorption isotherm, $\Gamma(c)$, we will use *empirical* isotherms, whose main merit is that they provide a very good fit of the experimental data.

Tajima (29) proposed an analytical expression for the equilibrium *adsorption* isotherm $c_1 = c_1(\Gamma)$ for aqueous solution of sodium dodecyl sulfate (SDS) with 0.115 *M* NaCl added, see also Ref. (14):

$$c_{10} = 2.1795 \times 10^{-5}\left(\frac{\Gamma_\infty}{\Gamma}\right)^{0.43} \times \frac{\Gamma}{\Gamma_\infty - \Gamma}\exp\left(\frac{\Gamma}{\Gamma_\infty - \Gamma}\right), \quad [5.1]$$

where $1/\Gamma_\infty = 25$ Å$^2$ and $c_{10}$ is expressed in mol/liter. To find the interfacial equation of state, i.e., $\sigma = \sigma(\Gamma)$ with $\sigma$ being the surface tension, we need a connection between $\sigma$ and $c_{10}$. As usual, we assume that the dependence of the surface tension on the subsurface concentration, $\sigma = \sigma(c_{10})$, is the same in equilibrium and nonequilibrium conditions. We measured the equilibrium ($c_{10} = c_{1\infty}$) dependence $\sigma = \sigma(c_{10})$ for SDS solutions with 0.115 *M* NaCl added. Then, following Mysels (30) we fitted the experimental dependence below CMC with a parabola in terms of $\log c_{10}$

$$\sigma(c_{10}) = -112.986 - 68.0136 \log c_{10} + 6.44987 \log^2 c_{10}, \quad [5.2]$$

where $c_{10}$ and $\sigma$ are expressed in mol/liter and mN/m, respectively. Equations [5.1] and [5.2] give the surface equation of state, $\sigma = \sigma(\Gamma)$, in a parametric form.

To see what our theoretical expectations are we first simulate the adsorption process in the experiments with the MBP method in the case of SDS solutions. For that purpose we assume that the bubble area increases linearly with time, viz.

$$A(t) = A_0\left(1 + 1.5\,\frac{t}{t_l}\right), \quad 0 \leqslant t \leqslant t_l, \quad [5.3]$$

where $t_l$ is the bubble lifetime. The latter dependence is close to the reality (see below). Then we substitute some relevant numerical values of the parameters for SDS as follows: $D_1 = 5.6 \times 10^{-6}$ cm$^2$/s and $D_m = 1.1 \times 10^{-6}$ cm$^2$/s, $m = 80$, $\Gamma_0 = 0$, $c_{10} = \text{CMC} = 10^{-3}$ mol/liter. Next, we start the numerical procedure described in the previous section; Eq. [5.1] plays the role of Eq. [1.1]. The numerical results for $\sigma$ vs $t_l$ simulated in this way are shown in Figs. 4a, b.

Figure 4a shows $\sigma$ vs $t_l$ curves for, $c_{m\infty} = 6.25 \times 10^{-6}$ mol/liter and three different values of the micellar decay rate constant $k_d$. As can be seen, the faster the micellar decay, the faster the relaxation of the surface tension. Such a dependence should be expected because the increase of $k_d$ leads to an increase of the source of monomers due to the presence of micelles.

Another factor leading to the same effect is the increase of the total surfactant concentration, $c_s = c_{1\infty} + mc_{m\infty}$, which results in an increase of $c_{m\infty}$ in so far as $c_{1\infty} = \text{CMC} = \text{const}$, see Fig. 4b. This is equivalent to an increase of the density of the sources of monomers, which, in turn, accelerates the relaxation of $\sigma$.

A similar study of the role of $k_d$ and $c_s$ on the relaxation of $\sigma$ has been carried out by Miller (31). For that purpose he solved the partial differential equations of diffusion for the case of an initial interfacial disturbance followed by surfactant diffusion toward quiescent, *nonexpanding* surface (i.e., the convection term $V_x \partial c/\partial x$ in Eqs. [2.3] and [2.5] is zero). Our results and his, about the role of $k_d$ and $c_s$, are qualitatively similar; quantitative coincidence should not be expected because of the difference in the processes simulated. It is interesting to note that the main difference is that Miller (31) established a pronounced effect of the ratio $D_m/D_1$ on the $\sigma$ vs $t_l$ curves, whereas such an effect does not appear in our calculations simulating the MBP method. The explanation is the following. The *convective* influx of micelles accompanying the surface extension in the MBP method turns out to be much more effective than the *diffusion* influx driven by the gradient of the micellar concentration, at least for the values of $t_l$ studied. Consequently, $D_m$ has no appreciable effect on the $\sigma$ vs $t_l$ curves in this case. In the case studied by Miller there is no convection, so the diffusion remains the only micellar supply.

The negligible effect of $D_m$ on the $\sigma$ vs $t_l$ curves, established by the above simulations of the MBP method for SDS solutions, has two additional consequences. For this system: (i) $D_m$ cannot be determined from the $\sigma$ vs $t_l$ curves by

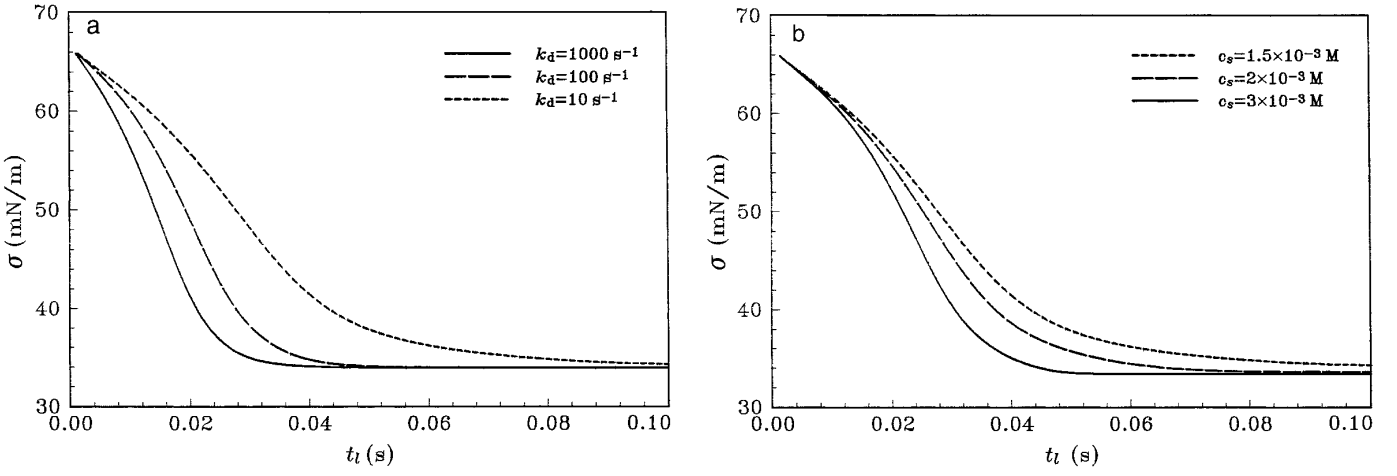


**FIG. 4.** Dynamic surface tension of micellar surfactant solution computed at (a) different values of the micelle decay rate constant $k_d$ and (b) different total surfactant concentration $c_s$. The other constants of the model are taken for SDS (containing 0.115 *M* NaCl): $c_s = 1.5 \times 10^{-3}$ mol/liter; $\Gamma_e = 4.29 \times 10^{-10}$ mol/cm$^2$; $D_1 = 5.6 \times 10^{-6}$ cm$^2$/s; $D_m = 1.4 \times 10^{-6}$ cm$^2$/s; $m = 80$.

analogy with the determination of $D_1$ from similar curves below CMC (14). (ii) The theory developed in Ref. (10) turns out to be applicable to the interpretation of data obtained by means of the MBP method. We recall that in Ref. (10) analytical expressions were derived at the cost of the assumption that $D_m \approx D_1$, which is not crucial as far as the results are not sensitive to $D_m$. In the Appendix we demonstrate that the theory from Ref. (10) gives satisfactory results even in the case of adsorption on a quiescent interface, when the ratio $D_m/D_1$ should be a physically essential parameter.

### 5.3. Comparison with Data of the MBP Method

First, we present results for SDS measured with three different surfactant concentrations above CMC in the presence of 0.128 *M* NaCl. CMC of this system is $c_{1\infty} = 1.08 \times 10^{-3}$ mol/liter. In this case, the increase of the bubble area with time was measured using a CCD camera for individual bubbles of different lifetimes $t_l$, see Fig. 5. Despite the different bubble lifetimes, the data for one and the same concentration are close to each other which is confirmed also for bubbles of smaller $t_l$, which are not shown in Fig. 5. All curves are of typical shape observed already for SDS solutions below CMC (24). Initially there is the sudden growth of a bubble which makes the bubble area $A$ different from the cross-sectional area of the capillary $A_c = \pi R_c^2$. Since the duration of this growth is less than the time resolution of our video system (0.033 s) we cannot say whether the bubble starts to grow from a flat interface, i.e., $A(0) = A_c$. After that, the bubble area increases almost linearly with time, and this gradual growth occupies the larger part of the bubble evolution; cf., Eq. [5.3]. Reaching hemispherical shape ($A = 2\pi R_c^2$) the bubble expands spontaneously and escapes from the capillary tip. This final stage of evolution is excluded from the computation of the dynamic surface tension (it is taken into account by the so-called dead time correction of the experimental data (24)).

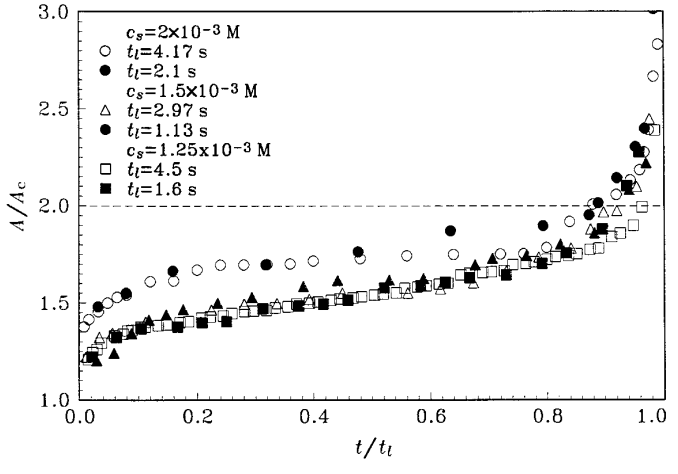


**FIG. 5.** Time dependence of the area $A$ of single bubbles of different lifetime $t_l$ blown in micellar solutions of SDS. The bubbles are formed on a hydrophobic glass capillary of hydrophilic tip (24) (capillary radius $R_c = 142$ $\mu$m).

By comparing the data of Tajima (29) for the surface adsorption isotherm, $\Gamma = \Gamma(c)$, with the expression proposed by him, Eq. [5.1], we reached the following conclusions. Equation [5.1] provides a good fit for $c < c' = 4.3 \times 10^{-5}$ mol/liter; for $c > c'' = 6.85 \times 10^{-4}$ mol/liter one can write $\Gamma = \Gamma_e = \text{const} = 4.29 \times 10^{-10}$ mol/cm$^2$. In the intermediate region, $c' < c < c''$, we fitted the data with an appropriate expression. Thus we obtained

$$\Gamma(c) = \begin{cases} \Gamma_T(c) & \text{for } c < c' \\ a_1 + a_2\sqrt{c} + a_3 c & \text{for } c' < c < c'' \\ \Gamma_e & \text{for } c > c'', \end{cases} \qquad [5.4]$$

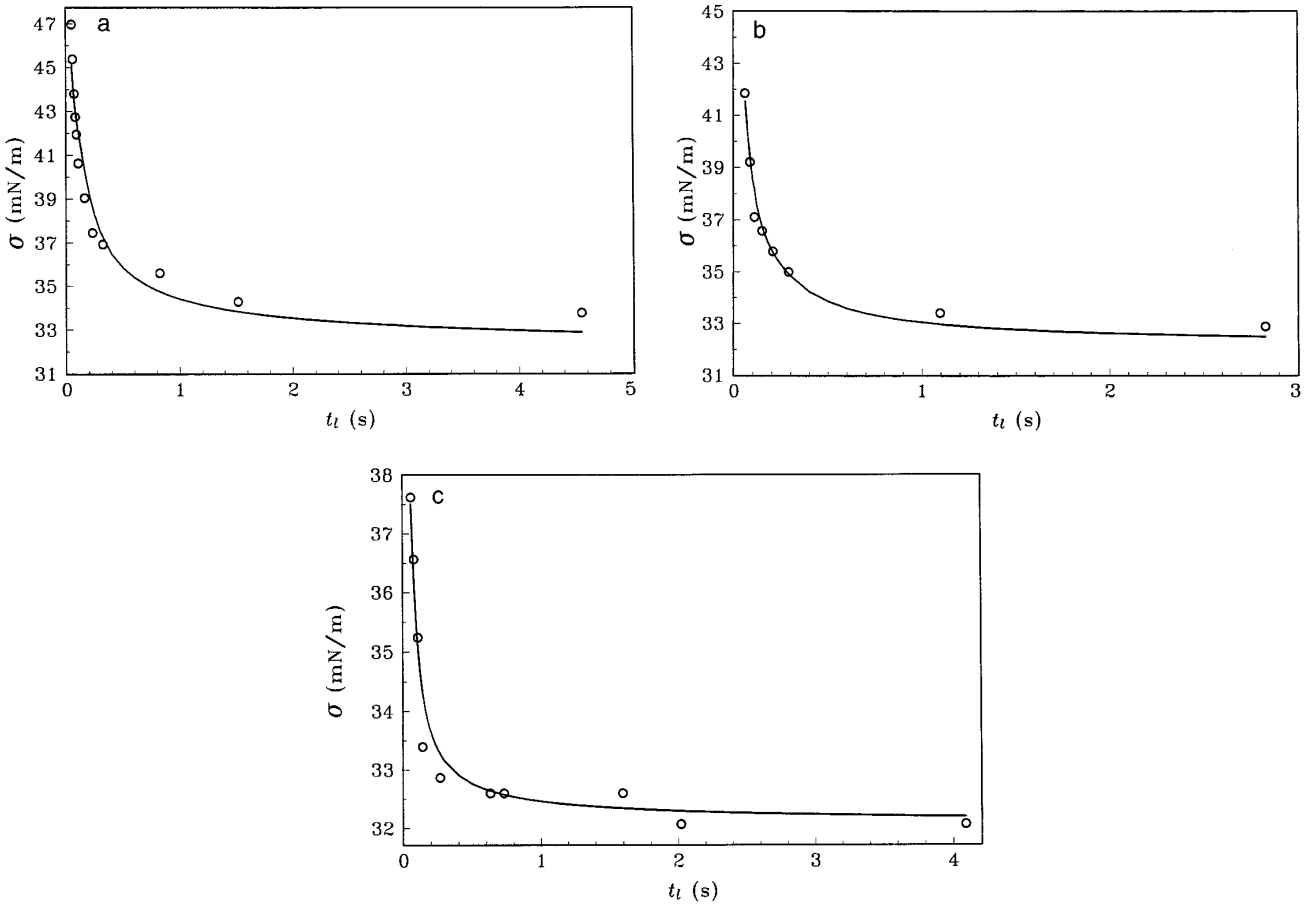


**FIG. 6.** Fits of experimental data for the dynamic surface tension of micellar solutions of SDS measured by the maximum bubble pressure method. Surfactant concentrations are: (a) $c_s = 1.25 \times 10^{-3}$ mol/liter; (b) $c_s = 1.5 \times 10^{-3}$ mol/liter; (c) $c_s = 2 \times 10^{-3}$ mol/liter. The constants are taken as $D_1 = 5.6 \times 10^{-6}$ cm$^2$/s (36); $D_m = 1.4 \times 10^{-6}$ cm$^2$/s; $m = 80$. The bubble area is shown in Fig. 5.

where $\Gamma_T(c)$ is determined by the Tajima expression, Eq. [5.1]. The constants $a_1$, $a_2$, and $a_3$ are determined by the conditions $\Gamma(c') = \Gamma_T(c')$, $\Gamma(c'') = \Gamma_e$, and $d\Gamma/dc = 0$ for $c = c''$. Equation [5.4] was substituted for Eq. [1.1] in our numerical calculations. The surface tension $\sigma$ was calculated from experimental data fits like Eq. [5.2]. As demonstrated above (Fig. 4a) $k_d$ (unlike $D_m$) affects considerably the $\sigma$ vs $t_l$ curves. Consequently, $k_d$ can be determined from these curves as an adjustable parameter. We applied the numerical procedure described in the previous section. Two adjustable parameters were used: $k_d$ and $\Gamma_0$, the latter being the adsorption in the initial moment of bubble formation ($t = 0$) which is not liable to be a direct measurement. The fits are shown in Figs. 6a–c for three total surfactant concentrations above CMC. The function $A(t)$ was taken to be an interpolation curve of the data shown in Fig. 5. The obtained values of the adjustable parameters $k_d$ and $\Gamma_0$ are listed in Table 1.

In the same way, we processed MBP data for aqueous solutions of sodium dodecyl polyoxyethylene-2 sulfate ($SDP_2S$) with 0.128 mol/liter NaCl added. The results for $c_s = 2 \times 10^{-4}$ mol/liter are shown in Fig. 7, where the circles represent experimental data for the dynamic surface tension measured by the MBP method (Vakarelski, I., private communication). The bubble area follows similar time dependence as the one depicted in Fig. 6 for SDS. The adsorption isotherm of $SDP_2S$ was calculated from experimental data for the equilibrium surface tension (Petkova, V., private communication) (CMC is $1.0 \times 10^{-4}$ mol/liter). The fit of the data by our theory is traced by solid line with parameters listed in Table 1. The theory agrees well with the experiment.

**TABLE 1**
**Parameters of Micellar Surfactant Solutions Calculated from Dynamic Surface Tension Data**

| Surfactant | $c$ mol/liter | $\Gamma_0/\Gamma_e$ | $k_d$ s$^{-1}$ |
|---|---|---|---|
| SDS | $1.25 \times 10^{-3}$ | 0.78 | 10.9 |
| | $1.5 \times 10^{-3}$ | 0.58 | 72.5 |
| | $2 \times 10^{-3}$ | 0.33 | 62.0 |
| $SDP_2S$ | $2 \times 10^{-4}$ | 0.73 | $8.5 \times 10^{-4}$ |

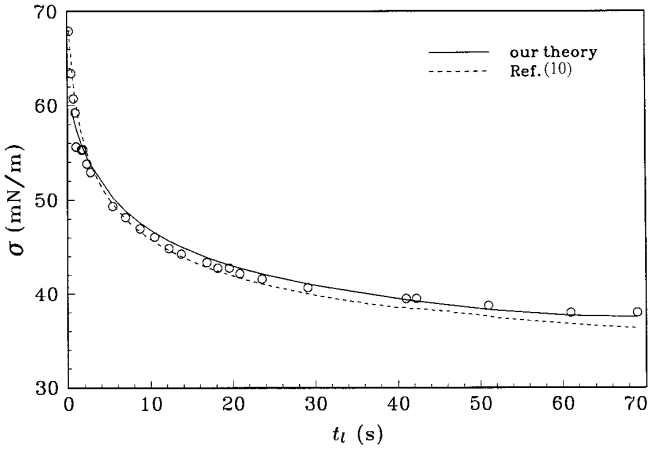


**FIG. 7.** Fit of experimental data for the dynamic surface tension of micellar solution of $SDP_2S$ at $c_s = 2 \times 10^{-4}$ *M*. The solid line is drawn by our theory with constants taken as $D_1 = 5.0 \times 10^{-6}$ cm$^2$/s; $D_m = 1.2 \times 10^{-6}$ cm$^2$/s (37); $m = 77$ (37). The dashed line is drawn by Eq. [A.1], see the Appendix.

The dashed line in Fig. 7 represents the fit drawn by means of the approximated theory in Ref. (10) (see Eq. [A.1] in the Appendix to the present article).

The values of the initial adsorption, $\Gamma_0$, listed in Table 1 are far from zero, which means that initially there is always adsorbed surfactant at the bubble surface. The values of the other adjustable parameter, $k_d$, given in Table 1, are discussed below.

### 5.4. Discussion

To judge the reliability of the values of the rate constant of micelle decay $k_d$ obtained by us for SDS we compare them with literature data available for homogeneous systems (kinetics of micellization). In this case the experiment gives the micellization time, $\tau_M$, directly while the rate constant $k_d$, as well as the micelle aggregation number $m$, are calculated after that by means of a model for the micellization kinetics. That is why two types of data for the rate constant are available in literature. The first type are data determined considering the simplified reaction pathway, Eq. [2.4], utilized also in our calculations. These are especially early papers on the kinetics of micellization (21, 32, 33) which interpret $\tau_M$ following the model proposed in Ref. (21). For example the rate constant of SDS solutions containing 0.1 *M* $NaNO_3$ obtained by temperature jump (T-jump) (33) is $k_d = 5.3$ s$^{-1}$ at temperature 35°C and micelle aggregation number $m = 95$. For SDS solution with no electrolyte added the respective values are $k_d = 30$ s$^{-1}$ and $m = 63$ as measured by pressure jump (p-jump) at 25°C (32). These data are close to the values for $k_d$ obtained by us from the dynamic surface tension of SDS solutions containing 0.128 *M* NaCl. On the same order is also the rate constant for another surfactant, dodecylpyridinium iodide, $k_d = 50$ s$^{-1}$ (21).

Although the values of $k_d$ determined by us should be one and the same for all concentrations, there is a difference in the values shown in Table 1. For SDS, the smallest value of $k_d$ obtained at $1 \times 10^{-3}$ mol/liter differs appreciably from the other two values which seem close to each other. This difference is most probably due to the oversimplified reaction scheme, Eq. [2.4], used. The experiments on micellization show that the relaxation in a micellar solution is characterized by two relaxation times (16, 17), which can be interpreted in the following way. The decay of a micelle is considered as a consequence of a *fast* and a *slow* process. The fast process is

$$A_m \overset{k_f}{\rightarrow} A_{m-1} + A_1, \quad m > n, \qquad [5.5]$$

where $k_f$ is the respective rate constant. In other words, for $m$ greater than a certain value $n$ a micelle can easily release a monomer and transform into micelle of aggregation number $m - 1$ without destruction of the micellar aggregate. In contrast, the detachment of a monomer from a micelle with the critical aggregation number $m = n$ leads to a breakup of the micelle into highly unstable fractions, which disintegrate to monomers. This is the slow process, which can be characterized by the equation

$$A_n \overset{k_s}{\rightarrow} nA_1. \qquad [5.6]$$

Here $k_s$ is the rate constant of the slow process, which can be c.a. 100 times smaller than $k_f$ (16, 17). Equations [5.5] and [5.6] characterize the decay of a micelle as a two-stage process.

Let us consider surfactant concentrations slightly above CMC, that is $c_{m\infty} \ll c_{1\infty}$. A decrease of the monomer concentration (caused e.g., by an expanding interface) will first start the fast process, Eq. [5.5]. As $c_{m\infty} \ll c_{1\infty}$, the monomers released by the fast process will not be enough to compensate for the shortage of monomers in the solution. Consequently, all micelles will quickly transform into critical $n$-aggregates, which will then decay by means of the slow process, Eq. [5.6]. In such a case, the micelle's decay will be controlled by the slow process, whose kinetic equation reads

$$\frac{dc_n}{dt} = -k_s c_n. \qquad [5.7]$$

Let $m$ be the mean aggregation number of the micelles at equilibrium. The experiment (34) shows that $m - n$ is about 5% of $m$. Then one can set $n \approx m$ in Eq. [5.7] and identify $k_d$ with $k_s$. The surfactant concentrations $c_s = 1.25 \times 10^{-3}$ mol/liter (Table 1) satisfies the condition $c_{m\infty} \ll c_{1\infty}$ (CMC $= 1.08 \times 10^{-3}$ mol/liter); hence, the respective value $k_d$ can be identified with $k_s$ for SDS, i.e., $k_s \approx k_d = 10.8$ s$^{-1}$. Measurements with the ''stop-flow'' technique (35) give $k_s$ of the same order of magnitude.

On the other hand, when $c_{m\infty} \geqslant c_{1\infty}$ the monomers released by the fast process, Eq. [5.5], will be enough to make up for the deficiency of monomers and therefore, the slow process, Eq. [5.6], will not be ''activated.'' Consequently, in such a case the source of monomers due to the micelles will be dominated by the fast process. Hence, one can expect that for larger surfactant concentration the effective rate constant $k_d$ will level off to a value determined by the fast process. The SDS data in Table 1 indicate that the latter value can be about 70 $s^{-1}$. To interpret this value we simplify Eq. [5.5] as

$$A_m \overset{k_f}{\rightarrow} A_n + (m - n)A_1. \qquad [5.8]$$

The respective kinetic equation reads

$$\frac{dc_1}{dt} = (m - n)k_f c_m. \qquad [5.9]$$

The latter is to be compared with the kinetic equation stemming from Eq. [2.4]:

$$\frac{dc_1}{dt} = mk_d c_m. \qquad [5.10]$$

Thus, one determines

$$k_f = \frac{m}{m - n} k_d. \qquad [5.11]$$

With $k_d = 70\ s^{-1}$ and $m/(m - n) = 20$, one calculates $k_f = 1400\ s^{-1}$. This seems to be a quite reasonable value, in so far as $k_f/k_s \approx 100$ is expected, see Refs. (16, 17).

The decrease of $\Gamma_0$ with the increase of $c_s$ (Table 1) is difficult to interpret. Most probably this is an artifact originating from an inadequacy in our model reaction scheme, Eq. [2.4], in comparison with the real two-stage process of micelle disintegration, cf., Eqs. [5.5] and [5.6].

As a concern to the result for $SDP_2S$, the value of $k_d$ listed in Table 1 is substantially smaller than the values for SDS. This value suggests much slower micellization kinetics for $SDP_2S$ than the common surfactants like SDS. This is not surprising bearing in mind that the adsorption of $SDP_2S$ is much slower (on the order of dozens of seconds) than the adsorption of SDS (tens of seconds) as it is seen in Figs. 6 and 7.

Finally, it should be noted that the reaction model based on Eq. [2.4], which we are using after Lucassen (8), is not a very essential part of our theoretical approach, whose most important steps are presented in Section 3 above. Indeed, one can apply the same ''von Karman's'' type of approach in conjunction with another reaction model. For example, it can be a reaction of ''*pseudo-first*'' *order,* which has been found by Joos and Van Hunsel (9) to compare well with experimental data. In fact, every reaction mechanism reduces to a reaction of ''pseudo-first'' order for small deviations from equilibrium, see e.g., Ref. (10), Section 5. This is the case with the experiments by Joos and Van Hunsel (9) carried out by means of the ''inclined plate'' and ''dynamic drop-volume'' methods.

On the other hand, the application of our theoretical approach makes sense for not too small deviations from equilibrium, like those observed with the MBP method. Otherwise, for small deviations the diffusion–adsorption problem becomes linear and one may apply the standard Laplace-transform technique (26).

## 6. CONCLUDING REMARKS

Our main goal in the present article is to develop a theoretical method describing the adsorption from micellar surfactant solutions. We developed a generalization of the approach from Ref. (14), which was initially designed for surfactant concentrations below CMC. The resulting numerical procedure turned out to be extremely fast and well convergent (see Section 4 above).

As an ingredient of the theory, we needed to introduce a reaction scheme of the micelle decay. As a first step we chose the most simple reaction scheme given by Eq. [2.4]. The rate constant of micelle decay, $k_d$, and the total surfactant concentration, $c_s$, were found to affect strongly the time dependence of surface tension, $\sigma(t_l)$, measured by the MBP method, see Fig. 4. In contrast, the micellar diffusion coefficient, $D_m$, does not affect appreciably the $\sigma(t_l)$ curves. This is a corollary of the fact that the convection accompanying the MBP experiment provides a more efficient supply of micelles than the diffusion.

Experimental data for $\sigma$ vs $t_l$ were fitted by means of our theoretical approach; $k_d$ was determined as an adjustable parameter. Concentration dependence of $k_d$ was established which can be attributed to the two-stage character of the micelle's decay. Until now time constants have been measured only by the so-called fast relaxation techniques of the chemical kinetics; p-jump, T-jump, or stopped flow. From an experimental point of view these bulk methods are more complicated than a surface stress experiment like the maximum bubble pressure method used by us. The sensitivity of the MBP measurements to the mechanism of micellar kinetics is an interesting finding, which stimulates us to extend this study in the future by including a more realistic (and more complicated) reaction scheme, like that based on Eqs. [5.5] and [5.6].

## APPENDIX

### Comparison with Analytical Solution

Here we compare our model with analytical solution for the surface tension for quiescent interface (10)

$$\frac{\Delta\sigma(t)}{\Delta\sigma(0)} = \frac{1}{2F}\exp(-\beta t)\left[(1+F)E\left(\frac{1+F}{2}\sqrt{\frac{t}{\tau_D}}\right) - (1-F)E\left(\frac{1-F}{2}\sqrt{\frac{t}{\tau_D}}\right)\right], \quad [A.1]$$

where $\Delta\sigma = \sigma - \sigma_e$; $E(x) = \exp(x^2)\mathrm{erfc}(x)$ is a function comprising the error function complement $\mathrm{erfc}(x) = 1 - \mathrm{erf}(x)$; $F = \sqrt{1+4\beta}$;

$$\beta = \frac{\tau_D}{\tau_M}$$

is the Damköhler number defined as the ratio of the characteristic diffusion time

$$\tau_D = \frac{1}{D_1}\left(\frac{d\Gamma_e}{dc_{1e}}\right)^2 \quad [A.2]$$

and the characteristic time of micellization $\tau_M$. In the model of micellar kinetics with one relaxation time $\tau_M$ is given by (21)

$$\tau_M = \frac{1}{k_d(1+m\theta)}, \quad \theta \equiv \frac{mc_{m\infty}}{c_{1\infty}}. \quad [A.3]$$

Equation [A.1] is derived (10) for nonexpanding interface, $\dot{\alpha} = 0$, assuming small deviations from equilibrium, $|1 - \xi_1| \ll 1$ and $|1 - \xi_m| \ll 1$, and nearly equal diffusivities of monomers and micelles, $D_1 \approx D_m$.

To simplify the respective equations in our model we expand the nonlinear terms in Eqs. [2.3] and [2.5] in series

$$c_1^m \approx c_{1\infty}^m[1 - m(1-\xi_1)]. \quad [A.4]$$

Then following the ideology from Section 3 we derive the equations

$$\frac{dl_1}{dt} = \left(\frac{\pi-2}{2}\right)\frac{D_1}{l_1}(1-\xi_1)^2 - l_1k_d(1+m\theta)$$

$$\frac{dl_m}{dt} = l_1k_d\frac{1+m\theta}{\theta},$$

which in dimensionless form read

$$\frac{dx_1}{dT} = \left(\frac{\pi-2}{2}\right)\frac{\xi_1^2}{x_1} - \beta x_1 \quad [A.5a]$$

$$\frac{dx_m}{dT} = \beta x_1, \quad [A.5b]$$

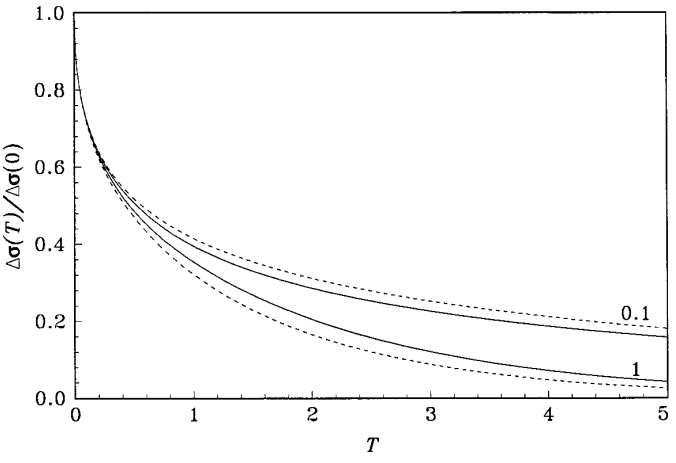


**FIG. 8.** Comparison between the predictions of our theoretical approach (solid lines) and Eq. [A.1] (dashed lines) for small deviations from equilibrium at $\beta = 0.1$ and $\beta = 1$.

where $T = t/\tau_D$ is dimensionless time. Equation [4.6] and the adsorption isotherm $\gamma = \gamma(\xi_1)$ can be written as

$$\gamma = x_1 + x_m \quad [A.6a]$$

$$\gamma = 1 - \frac{d(\ln\Gamma_e)}{d(\ln c_{1e})}(1-\xi_1). \quad [A.6b]$$

Equations [A.5] and [A.6] are solved numerically to obtain the surface tension as a function of dimensionless time $T = t/\tau_D$ shown in Fig. 8 for two different values of $\beta$. The curves calculated by our approach in Section 3 above (the solid lines) are in close agreement with the analytical solution [A.1] (the dashed lines). The deviation at large $T$ can be due to the fact that some of the approximations made in our model become substantially different than the approximations made in deriving Eq. [A.1].

## ACKNOWLEDGMENTS

The authors are indebted to Dr. N. D. Denkov for the helpful discussions and to Mrs. E. Basheva and Mr. I. Vakarelsky for performing part of the measurements of dynamic surface tension. The financial support of Colgate–Palmolive is greatly acknowledged.

## REFERENCES

1. Defay, R., and Pétré, G., *in* ''Surface and Colloid Science'' (E. Matijevic, Ed.), Vol. 3, p. 27. Plenum, New York, 1971.
2. Van Voorst Vader, F., Erkens, Th. F., and Van den Tempel, M., *Trans. Faraday Soc.* **60,** 1 (1964).
3. Lange, H., *J. Colloid Sci.* **20,** 50 (1965).
4. Joos, P., and Rillaerts, E., *J. Colloid Interface Sci.* **79,** 96 (1981).
5. Miller, R., and Lunkenheimer, K., *Colloid Polymer Sci.* **264,** 357 (1986).
6. Lucassen-Reynders, E. H., *J. Phys. Chem.* **70,** 1777 (1966).
7. Davies, J., and Riedel, E., ''Interfacial Phenomena.'' Academic Press, New York, 1963.

8. Lucassen, J., *J. Chem. Soc. Faraday Trans. 1* **72,** 76 (1976).
9. Joos, P., and Van Hunsel, J., *Colloids Surf.* **33,** 99 (1988).
10. Dushkin, C. D., Ivanov, I. B., and Kralchevsky, P. A., *Colloids Surf.* **60,** 235 (1991).
11. McCoy, B. J., *Colloid Polymer Sci.* **261,** 535 (1983).
12. Miller, R., *Colloid Polymer Sci.* **259,** 375 (1981).
13. Rakita, Yu. M., Fainerman, V. B., and Zadara, V. M., *Zh. Fiz. Khim.* **60,** 376 (1986). [in Russian]
14. Kralchevsky, P., Radkov, Y., and Denkov, N., *J. Colloid Interface Sci.* **161,** 361 (1993).
15. Batchelor, G. K., ''An Introduction to Fluid Dynamics.'' Cambridge Univ. Press, Cambridge, UK, 1970.
16. Aniansson, E. A. G., Wall, S. N., Almgren, M., Hoffmann, H., Kielmann, I., Ulbricht, W., Zana, R., Lang, J., and Tondre, C., *J. Phys. Chem.* **80,** 905 (1976).
17. Aniansson, E. A. G., and Wall, S. N., *J. Phys. Chem.* **78,** 1024 (1974); *J. Phys. Chem.* **79,** 857 (1975).
18. Dushkin, C. D., and Ivanov, I. B., *J. Surface Sci. Technol.* **6,** 269 (1990).
19. Noskov, B. A., *Kolloidn. Zh.* **52,** 509 (1990); *Kolloidn. Zh.* **52,** 796 (1990). [in Russian]
20. Dushkin, C. D., and Ivanov, I. B., *Colloids Surf.* **60,** 213 (1991).
21. Kresheck, G., Hamori, E., Davenport, G., and Scheraga, H., *J. Am. Chem. Soc.* **88,** 246 (1966).
22. Feinerman, V. B., and Rakita, Yu. M., *Kolloidn. Zh.* **52,** 106 (1990). [in Russian]
23. Iliev, Tz. H., and Dushkin, C. D., *Colloid Polymer Sci.* **270,** 370 (1992).
24. Horozov, T. S., Dushkin, C. D., Danov, K. D., Arnaudov, L. N., Velev, O. D., Mehreteab, A., and Broze, G., *Colloids Surf.*, in press.
25. Rillaerts, E., and Joos, P., *J. Phys. Chem.* **86,** 3471 (1982).
26. Dushkin, C. D., Iliev, Tz. H., Radkov, Y. S., *Colloid Polymer Sci.* **273,** 370 (1995).
27. Joos, P., and Rillaerts, E., *J. Colloid Interface Sci.* **70,** 96 (1981).
28. Garrett, P. R., and Ward, D. R., *J. Colloid Interface Sci.* **132,** 475 (1989).
29. Tajima, K., *Bull. Chem. Soc. Japan* **43,** 3063 (1970).
30. Mysels, K. J., *Langmuir* **5,** 442 (1989).
31. Miller, R., *Colloid Polymer Sci.* **259,** 1124 (1981).
32. Janjic, T., and Hoffmann, H., *Z. Phys. Chem., Neue Folge* **86,** 322 (1973).
33. Bennion, B. C., Tong, L. K. J., Holmes, L. P., and Eyring, E. M., *J. Phys. Chem.* **73,** 3288 (1969).
34. Chan, S.-K., Herrmann, V., Ostner, W., and Kahlweit, M., *Ber. Bunsenges. Phys. Chem.* **81,** 60 (1977).
35. Kahlweit, M., and Teubner, M., *Adv. Colloid Interface Sci.* **13,** 1 (1980).
36. Kamenka, N., Lindman, B., and Brun, B., *Colloid Polymer Sci.* **252,** 144 (1974).
37. Alargova, R., Petkov, J., Petsev, D., Ivanov, I. B., Broze, G., and Mehreteab, A., *Langmuir* **11,** 1530 (1995).